The Integrative Approach to Study of the Structure and Functions of Cardiac Voltage-Dependent Ion Channels

Juila G Kacher, Maria G Karlova, Grigory S Glukhov, Han Zhang, Elena V Zaklyazminskaya, Gildas Loussouarn, Olga S. Sokolova

▶ **To cite this version:**

Juila G Kacher, Maria G Karlova, Grigory S Glukhov, Han Zhang, Elena V Zaklyazminskaya, et al.. The Integrative Approach to Study of the Structure and Functions of Cardiac Voltage-Dependent Ion Channels. 2021. hal-03350105

HAL Id: hal-03350105

https://nantes-universite.hal.science/hal-03350105

Preprint submitted on 21 Sep 2021

HAL is a multi-disciplinary open access archive for the deposit and dissemination of scientific research documents, whether they are published or not. The documents may come from teaching and research institutions in France or abroad, or from public or private research centers.

L'archive ouverte pluridisciplinaire **HAL**, est destinée au dépôt et à la diffusion de documents scientifiques de niveau recherche, publiés ou non, émanant des établissements d'enseignement et de recherche français ou étrangers, des laboratoires publics ou privés.

REWIEW

УДК 577.25

THE INTEGRATIVE APPROACH TO STUDYING STRUCTURE AND FUNCTIONS OF CARDIAC VOLTAGE-DEPENDENT ION CHANNELS

(c) 2020 Kacher Y.G.[1], Karlova M.G.[1], Glukhov G.S.[1], Zhang H.[2] Zaklyazminskaya E.V.[3], Loussouarn G.[4], Sokolova O.S.[1,2]*

[1] *Lomonosov Moscow State University, Faculty of Biology, Moscow, Russia*

[2] *MSU-BIT University in Shenzhen, Shenzhen, China*

[3] *Petrovsky Russian Scientific Center of Surgery, Moscow, Russia*

[4] *L'unité de recherche de l'institut du thorax, Inserm, CNRS, France*

**e-mail: sokolova@mail.bio.msu.ru*

Received

Annotation

Membrane proteins, including ion channels, became the focus of structural proteomics in the mid-20th century. The methods for studying ion channels are diverse and include structural (X-ray crystallography, cryoelectron microscopy, X-ray free electron lasers) and functional (e.g. patch clamp) methods. This review highlights the evolution of approaches to study the structure of cardiac ion channels, provides an overview of new techniques of structural biology applying to ion channels, including the use of lipo- and nanodiscs, and discusses the contribution of electrophysiological studies and molecular dynamics to obtain a complete picture of the structure and functioning of cardiac ion channels. Electrophysiological studies have become a powerful tool for deciphering the mechanisms of ion conductivity and selectivity, gating and regulation, as well as testing molecules of pharmacological interest. Obtaining of the atomic structure of ion channels was made possible by the active development of X-ray crystallography and cryoelectron microscopy, and recently by the use of XFEL.

Key words: voltage-dependent ion channels, channelopathies, heart diseases, structural biology, electrophysiology, protein purification, nanodiscs, lipodiscs, cryoelectron microscopy, X-ray crystallography, X-ray free electron lasers.

INTRODUCTION **2**

1. CARDIAC ION CHANNELS AND CHANNELOPATHIES: WHY DO WE NEED TO KNOW THE STRUCTURE OF ION CHANNELS? 3
2. PATH TOWARDS THE STRUCTURE OF A FULL-SIZE ION CHANNEL 5
3. STRUCTURAL-FUNCTIONAL INVESTIGATIONS OF ION CHANNELS 6
4. ELECTRON MICROSCOPY FOR THE INVESTIGATION OF ION CHANNELS 8
5. REVOLUTION IN STRUCTURAL BIOLOGY - CRYO-EM STRUCTURES OF ION CHANNELS WITH NEAR-ATOMIC RESOLUTION 8
6. NEW STRATEGIES FOR THE PURIFICATION OF ION CHANNELS 10
   6.1. Why is it so difficult to study structure of membrane proteins? *10*
   6.2. Nanodiscs *11*
   6.3. Lipodiscs *12*
7. STUDY OF ION CHANNEL DYNAMICS USING X-RAY FREE ELECTRON LASERS 13

CONCLUSIONS **14**

LITERATURE **24**

INTRODUCTION

The 20th century was a blossom of structural biology - an enormous amount of structural data was obtained and a real potential for reconstructing all processes in living organisms was accumulated. Two decades of the 21st century have come to an end with more than 160,000 tertiary and quaternary protein structures deciphered; these include large molecular machines, ribosomes [1], membrane proteins [2, 3], cytoskeleton proteins [4], enzymes, etc. Optimists predict solving the structures of all known proteins and their functions in 30 years. This means not only understanding the structure of individual macromolecules and their interactions with ligands, but also intermolecular interactions in protein complexes. Conformational changes in a protein reflect its functional activity [5]. Comprehensive knowledge of the structures of a protein molecule makes it possible to correctly interpret its conformational changes during activation and inhibition and learn how to control these processes [6].

Following genomics, proteomics, transcriptomics and metabolomics, a ‘structural proteomics’ emerged. Understanding biological mechanisms at the atomic level allowed to apply this information in medicine and biotechnology. This is relevant for the study of membrane proteins, in particular ion channels and transporters, which take part in regulating the vital functions of every cell in the body, especially cardiomyocytes.

Ion channels are a large functional class of integral transmembrane proteins. Most ion channels have a rotational symmetry formed by several identical subunits or homologous domains around the channel pore. Ion channels can be classified by their gating mechanism: voltage-gated, ligand-gated, light-gated, mechanosensitive, cyclic nucleotide-gated and calcium-gated ion channels.

Voltage dependent (**VD**) ion channels are the most extensive group. Their role in excitable cells is to depolarize or repolarize the membranes in response to changes in potential. The structural unit of most of the VD channels conducting K^+, Ca^{2+} and Na^+ ions consists of four subunits or four transmembrane domains, each formed by six helixes (Fig. 1B), crossing the lipid bilayer. Their functioning is determined by the coordinated operation of three structural units: voltage sensor (helixes 1 to 4), pore and channel gate (helixes 5 and 6, Fig. 1A and 1B).

Action potentials (**AP**) in heart cells differ significantly from those found in other cell types. This is due to the presence of heart-specific ion channels (mostly expressed in cardiomyocytes) and specific kinetics of their work. Rapid Nav channels are responsible for the depolarization of the myocyte membrane while the Cav ion channels are responsible for the plateau phase. Kv channels play a crucial role in determining the resting potential and the phase of repolarization (Figure 1B).

1. Cardiac ion channels and channelopathies: why do we need to know the structure of ion channels?

The rhythmic contraction of the heart throughout a person's life course is provided by synchronous generation and propagation of electrical impulses provided by the well-coordinated operation of several dozen ion channels. Voltage-dependent cation channels and accessory proteins encoded by the *KCNQ1*, *KCNH2*, *KCNE1*, *KCNE2*, *KCNJ2*, and *TRPM4* genes play an important role in the repolarization of cardiac cells and the maintenance of normal duration of cardiac AP.

The Kv7.x or KCNQ family includes five channel types (Kv7.1 - Kv7.5). The Kv7.1 channel, encoded by the *KCNQ1* gene, is predominantly expressed in the cardiac tissue, as well as in the epithelial tissue and smooth muscles. Kv7.2-Kv7.5 (*KCNQ2-5*) channels are mainly found in the nervous system [7]. In cardiac the muscle, Kv7.1 is expressed together with the accessory *KCNE1*, *KCNE2*, and *KCNE3* beta-subunits to form a functionally active channel that provides a slow repolarization current [8], and, therefore, is responsible for the duration of cardiac AP. To date, more than 100 mutations (mainly single nucleotide variations, SNV) are described affecting the activity of the Kv7.1 channel, altering the kinetics of activation and interaction with regulatory subunits, or disrupting traffic to the cell membrane. These alterations lead to the development of

a prolonged QT interval (Type 1 Long QT syndrome, LQTS) on the electrocardiogram (ECG) (Fig. 1D) and may manifest as a sudden cardiac death (SCD). In addition to LQTS, some of these mutations are associated with recessive Jervell and Lange-Nielsen syndrome [9], a condition in which heart rhythm disturbances are accompanied by hearing impairment. For this channel, activating mutations that cause an increase in current and lead to a shortening of the AP duration (Short QT syndrome, short QT, SQT) and atrial fibrillation [10] are also described.

The correct functioning of ion channels can be impaired by mutations that affect the number of expressed protein subunits, primary and secondary structure, and protein post-translational modifications. As a result of genetically determined changes, the total ion permeability through the channel can increase (one of the two gates, activation or inactivation gate, is more frequently open at a given potential, protein expression increases), or decrease (one of the two gates, activation or inactivation gate, is more frequently closed at a given potential, protein expression increases). It is noteworthy that mutations differing in their functional effect can lead to clinically opposite electrocardiographic phenomena, and the corresponding arrhythmogenic syndromes form an allelic series of diseases. The well-studied examples of an allelic series of diseases are syndromes that develop as a result of various mutations in the *KCNH2* gene. Loss-of-function mutations (for example, substitutions of N410D, A561T, G610S, A614V, N996I, etc.) lead to a decrease in the total outgoing potassium current from the cell, which delays repolarization and is expressed by QT prolongation [11]. This genetic form is the second most common subtype of hereditary LQTS (Type 2 LQTS), a disease with a high risk of developing “torsade de pointes” type ventricular tachycardia and sudden cardiac death [12]. Mutations in this gene account for about 35% of all genetically confirmed cases of the LQTS [13].

Gain-of-function *KCNH2* mutations lead to an increased outward flux of positively charged potassium ions which results in acceleration of repolarization and is manifested by abnormally short QT intervals on the ECG (Fig. 1D). The electrocardiographic and clinical manifestations of such mutations are more diverse, and include short QT syndrome (T618I replacement), Brugada syndrome (eg, T152I, R164C, W927G, R1135H, etc.), familial atrial fibrillation (N588K variant) [14-16].

The functioning of the Kv11.1 channel (encoded by the *KCNH2* gene) can be altered not only by mutations, but also by interactions with a wide range of drugs. The blocking of the Kv11.1 channel with the development of secondary cardiac AP duration lengthening (and, as a consequence, prolongation of the QT interval) is one of the very dangerous side effects of a wide range of drugs. Terfenadine, a histamine H1-receptor antagonist, was the first drug in 1998 withdrawn from the pharmacological market due to the blockade of the Kv11.1 channel and the risk of ventricular arrhythmias was, and now there are at least a dozen of such drugs [17].

Currently, all new pharmaceutical substances are being tested for their ability to block cardiac ion channels, mainly Kv11.1. Understanding the structure and functioning of ion channels (Kv11.1 in particular) is very important for the rational design of new drugs of any kind. It was shown that some amino acids in the S6 domain (Tyr652, Phe656) and at the base of the pore helix (Thr623, Ser624, Val625) are especially susceptible to drug interactions [18]. Regardless of the direction in which the duration of cardiomyocyte repolarization is shifted, the main threat to carriers of mutations in the *KCNH2* gene is an increased risk of developing ventricular arrhythmias and sudden death.

The effectiveness of the treatment of various inherited cardiac channelopathies is different. Currently, both surgical (implantation of antiarrhythmic devices and left stellectomy) and conservative approaches are available. Beta-blockers have shown high but not absolute efficiency in LQTS treatment [19]. However, such drug therapy is insufficient for other channelopathies (such as familial cardiac conduction disease (CCD), Brugada Syndrome (BrS), short QT syndrome (SQTS)). Therefore, a detailed study of structural and functional changes in normal and mutant ion channels is necessary for the development of new molecules capable of compensating for the genetic defect.

New generation sequencing has led to an exponential increase in the number of genetic tests performed. A natural result of the growth of conducted diagnostic tests was the identification of a large number of new, uncharacterized rare variants, the clinical significance of which is difficult to interpret. A detailed understanding of the structure of ion channels, understanding of the functional significance of each amino acid residue will help develop predictive models that can reliably predict the importance of new unique variants.

2. Path towards the structure of a full-size ion channel

By the end of the 20th century, many genes encoding eukaryotic ion channels as well as their bacterial analogues had been successfully cloned. However, the quaternary structure of most of the ion channels remained unknown for a long period of time, since they hardly crystallize. Conclusions about the structure and functioning of the channels were made based on indirect data from mutation analysis, electrophysiology and molecular dynamics (**MD**) (Fig. 2A-G).

In the absence of direct structural data, comprehensive approaches were developed to solve the difficult task of determining the processes underlying the activation of Kv channels. This problem was partly solved by the early 90s of the 20th century, when the first models of Kv channels activation were proposed (reviewed in [26]). According to cysteine scanning and electrophysiology data, it has been demonstrated that i) the Kv channel forms a tetrameter (Fig. 2A); ii) in response to membrane depolarization, the S4 voltage sensor moves across the membrane

[27] and, iii) the S4 helix pulls the S4-S5 linker, which leads to a disturbance of the S4-S5/S6 interaction and finally to the opening of the channel pore [28] (Fig. 3A). However, some activation models were later found to be controversial [29]. Real structural data were needed to validate them.

The first crystal structure of the KcsA bacterial (*Streptomyces lividans*) ion channel with 3.2 Å resolution was obtained in the laboratory of the future Nobel Prize winner R. MacKinnon and published in 1998 [21]. This work has been cited more than 7000 times over the past 22 years. Since the pore structure is homologous in most cation channels [30], the KcsA structure has opened up invaluable opportunities for structural biologists and biophysicists (Fig. 4).

The atomic structure of KcsA allowed MD to model its own conformational dynamics [31], but also those of homologous eukaryotic channels [32, 33] (Fig. 3B). To get the 1998 structure, authors removed intracellular C-terminal parts of the KcsA protein to obtain well-diffracting crystals. It was therefore crucial to prove the functionality of the obtained structure - the renaissance of electrophysiology began.

3. Structural-functional investigations of ion channels

The fundamental understanding of how the structure of cation channels is altered by mutations is possible only if the structural studies are combined with functional (electrophysiological) approaches. Characterization of ion channel activity, by the use of electrophysiology, is the chief source of knowledge in both physiological and pathophysiological contexts, which, in turn, helps in the development of drugs.

In the 20th century, electrophysiology shed light on molecular mechanisms of conduction, selectivity, gating, and on the regulation of ion channels by accessory protein [34-39].

Regarding ion channel pathophysiology, electrophysiological tools, in particular the patch-clamp technique [40], were used in thousands of studies to confirm gene variants as being the cause of the pathology. A good example is the long QT syndrome, a cardiac disorder characterized by ventricular fibrillation, and an increased risk of sudden cardiac death (cf. above). The rather simple scheme of monogenic transmission of the disease is probably the reason why it was one of the inherited diseases under focus early on, after the identification of several genes coding for the incriminated ion channels, mainly *KCNQ1*, *KCNH2*, and *SCN5A* [41, 42]. In many biophysical studies, the identified mutation was introduced in a plasmid coding for a channel, and patch-clamp experiments were undertaken, to test if the mutation leads to a modification of the current.

After the golden age of these ‘simple’ models, and benefiting from major advances in high throughput sequencing and genomic analyses, research has gradually moved on to more complex modes of inheritance diseases such as the Brugada syndrome [43]. This syndrome is also a cardiac disorder characterized by ventricular fibrillation and increased risk of sudden cardiac death, as in

the long QT syndrome, but the pathophysiology is somewhat different: ECG monitoring easily distinguishes long QT syndrome (prolonged QT interval) from Brugada syndrome (ST segment elevation). In the long QT syndrome, most of the cases have been linked to a specific mutation, mainly in *KCNQ1*, *KCNH2*, and *SCN5A* genes. In Brugada syndrome, a mutation in a gene has been identified in only 20% of Brugada patients, in spite of the clear familial origin of the pathology. Even more complex, in many cases when a gene mutation has been identified in a family (mainly *SCN5A*, coding for the voltage-gated sodium channel Nav1.5), some members of the family present the mutation but not the pathology (incomplete penetrance), some members present the pathology but not the mutation (phenocopy) [44]. In that condition, electrophysiology tools such as patch-clamp were of great interest, even greater than for the long QT syndrome, to study if the identified mutation led to a dysfunction of the channel and may at least partially participate to the pathogenesis.

Still, regarding ion channel pathophysiology, electrophysiology tools also represent instrumental support to delineate how disruption of a given molecular mechanism may lead to a given pathology. For instance, patch-clamp studies showed that Kv7.1 and Kv11.1 voltage-gated channels activity requires the phospholipid phosphatidylinositol (4,5) bisphosphate ($PI(4,5)P_2$) and that some long QT mutations alter the interaction of $PI(4,5)P_2$ with the channel and lead to a loss of channel function [45-47].

Last, looking at the intimate intramolecular interaction in voltage-gated channels, with patch-clamp led to design peptides mimicking these interactions and either inhibiting or activating ion channels [48-51]. Such a study may lead in the long term, to a new therapeutic avenue.

In all these aforementioned aspects, the development of high throughput patch-clamp tools will be helpful. First, the major interest of functional validation of variants, mentioned above, combined with the rapid increase of gene variants to be tested, more than 1000 in Kv11.1 (hERG) channel, motivates the development and use of such high throughput gene phenotyping. This tool also starts to be exploited for drug screening [52, 53].

It is also important to mention the limitations of patch-clamp, especially because it may lead to misinterpretation regarding the function of proteins. A typical case is the story of KCNE1, originally named MinK (minimal potassium channel) because it was wrongly supposed to be an ion channel, based on the observation that its expression in Xenopus Oocyte led to a slowly activating voltage-gated potassium current. Despite cautious interpretation in the first article, complementary experiments tended to confirm this hypothesis [54, 55]. But the slowly activating voltage-gated current channel could only be observed when the mRNA was injected in Xenopus Oocytes, but not other models, raising some doubts about the gene really encoding an ion channel [56]. Cloning of the right gene, *KCNQ1* (named *KvLQT1* originally), and demonstration that it is

also present in Xenopus Oocytes and generate a slowly activating voltage-gated current only in presence of KCNE1 definitely demonstrated that KCNE1 was not coding for the pore-forming subunit [38, 39].

4. Electron microscopy for the investigation of ion channels

In the nineties, electron microscopy started to be used to study the structure of ion channels. The channels were isolated from cell membranes using detergents (DDM, CHAPS, digitonin and others), applied to the carbon-coated grids and contrasted with heavy metal salts (Fig. 2D) [24, 57-60], or studied by cryoelectron microscopy (**cryo-EM**) [61, 62].

The advantage of cryo-EM is that protein molecules are in a water environment, so their shape and conformation are preserved. The particles in vitrified ice may not have priority orientation, comparing to the particles on the carbon surface. At the same time, the signal-to-noise ratio in cryo-EM is generally low, because of low contrast of the protein molecules. In order to increase contrast, data from a very large number of projections are combined. The reconstructions of macromolecules based cryo-EM data has been used for over four decades now, but in the initial stages it was possible to obtain three-dimensional structures with a moderate resolution of 15-18 Å only for large ion channels such as the ryanodine- receptor (RyR) [63, 64].

Radiation damage is a significant barrier to obtaining high-resolution reconstructions [65]. To reduce radiation damage, the low dose systems are used in order to block the beam during the selection of the survey area, alignment and focusing of the electron beam until the last step - obtaining the image. Small exposures result in loss of resolution, noisy images and, as a result, lack of high-resolution data. This, in turn, complicates the subsequent image processing to determine the three-dimensional structure of an object. Determining the Euler angles for globular molecules is particularly sensitive to noise in raw images and to errors in alignment and classification procedures. Small size of Kv channel molecules (10-15 nm in diameter) led to loss of image contrast in the microscope and a low resolution of reconstruction.

For very short exposures, the ability of the detector to perceive every electron becomes critical. Such devices were designed in the 21st century which allow direct detection of electrons (direct detector of electron, **DDE**) and obtaining 16 to 400 frames per second exposure. Due to a special image processing procedure, motion correction, same images from all frames can be aligned with each other and summarized to increase the signal-to-noise ratio. This compensates for the movement of the particles in the ice, which occurs during a second exposure time [66].

5. Revolution in structural biology - cryo-EM structures of ion channels with near-atomic resolution

In the 15 years since the publication of the first crystal structure of the ion channel, researchers have been able to decipher the atomic structure of a number of prokaryotic [21, 67, 68], archean [69] and eukaryotic (e.g. Fig. 2E) ion channels using X-ray crystallography [70-72].

The revolution in the structural biology of membrane proteins began with the publication in 2013 the first atomic structure of the TRP ion channel [73], *de novo* obtained using cryo-EM, which, in particular, is associated with the beginning of serial production of DDE. The development of new 3D-reconstruction software [74] has tremendously accelerated the collection and analysis of hundreds of thousands to millions of images of individual channel particles. In 2015, the cryo-EM method was declared the method of the year by Nature magazine, and two years later, in 2017, three founding scientists of the method - R. Henderson, J. Dubochet and J. Frank - were awarded the Nobel Prize. And that was just the beginning. Over the next 7 years, a technical breakthrough allowed many previously unknown structures of ion channels to be deciphered, including the cardiac channel and its accessory subunit KCNQ1 and KCNE2 [75, 76].

The first high-resolution cryo-EM studies of the EAG family channel revealed that the activation model based on data on the structure of *Shaker* family channels [26, 77] was not suitable for describing the activation of the channels encoded by the *KCNH* genes [3, 49, 75, 78]. The structure of the membrane domain of *Shaker* family channels has a characteristic feature, which became clear after deciphering the first crystal structure of the chimeric channel Kv1.1/Kv1.2 [71]: its VSD interacts not with its own pore domain, but with a domain belonging to a neighboring subunit (Fig. 5A, B). Such architecture was called "domain swapped". This arrangement of transmembrane helixes was possible because of the long S4-S5 linker in the *Shaker* family channels. The domain swapped architecture was not applicable to EAG channels because of a very short S4-S5 linker; therefore, its S5 helix interacts with its own VSD (Figure 5B, D) [75].

A comparison of the open conformations of the chimeric Kv1.2/2.1 [71] and Kv11.1 [3] channels to the closed conformation of the Kv10.1 channel, due to interaction with calmodulin (**CaM**) [75], led researchers to a new hypothesis of the EAG family channels functioning (Fig. 6). The difference from the previous model is that the S4-S5 linker is given a smaller role, and the main change in the conformation of S6 is due to lateral displacement of S4 and S5 segments. The hinge that provides the conformation change of S6 is formed by two Glycines: G648 in Kv11.1 and G460 in Kv10.1 [3].

In parallel, it has been suggested that the activation of EAG family channels takes place via so-called ligand-receptor mechanism (Fig. 3B). In this case, the S4-S5 linker acts as an internal ligand that binds the lower part of the S6 helix and locks the channel in a closed state when the S4 VSD helixes are in a "down" state with negative potential. When the S4 helixes transit to the "up" state, the S4-S5 linker leaves its binding pocket on the S6 and the channel is opened. This

molecular mechanism is in good agreement with the results of electrophysiological experiments [79] obtained, in particular, on hERG channels [49].

6. New strategies for the purification of ion channels

6.1. Why is it so difficult to study structure of membrane proteins?

Structural studies require the production of the target protein in large quantities and with a high degree of purity. Nowadays many different approaches to the production and purification of proteins have been developed. However, for membrane proteins, it is the sample preparation that is the bottleneck in determining the structure, in particular the extraction of the target protein from cell membranes. A detergent that improperly mimics the hydrophobic environment of the protein of interest can also significantly alter its structure.

Under such conditions, 30 years ago, electronic crystallography could only achieve the subnanometer resolution: the structures of bacteriorhodopsin in the purple membrane [80] and the acetylcholine receptor in the electric organ of the *Torpedo marmorata* [81] were obtained using this method. Later, it became possible to simulate natural two-dimensional crystals, instead of native membranes, using purified channel molecules and, by dialysis, removing the detergent from the mixture, replacing it with lipids, but this approach turned out to be quite difficult to reproduce and is still used in only a few laboratories in the world.

To obtain reconstructions of channel proteins in the membrane environment, other special approaches have also been developed, such as, for example, spherical reconstruction [82]. After insertion into a small spherical lipid vesicle, the membrane protein acquired a strictly defined orientation relative to the membrane, and its position on the projected image of the vesicle directly determined two of the three determined Euler angles. Analysis of images of vesicles in ice showed that their density is well described by a simple model of electron scattering on a membrane. Computer simulations have shown that this method can theoretically improve the reconstruction of membrane proteins. We applied it to study the clustering of gramicidin in liposomes [83]; however, the method did not allow achieving high resolution.

The importance of lipids of the nearest environment has been shown for many proteins, for example, the interaction of $PI(4,5)P_2$ with Kv7 [45] and the interaction of KscA with anionic lipids [84]. Removal of these lipids upon solubilization with detergents can lead not only to functional impairments, but also to structural rearrangements. In this regard, both the search for new detergents and the development of fundamentally new approaches to the solubilization of membrane proteins are constantly being carried out. Relatively recently, two similar, but based on

different compounds, approaches have been developed - the use of nanodiscs and lipodiscs in structural studies of membrane proteins.

6.2. Nanodiscs

Nanodiscs represent an alternative and more efficient approach to the isolation of membrane proteins. These are simulators of the membrane environment (membrane mimetics) that can be used to maintain membrane proteins in a soluble form for further structural studies. As the name suggests, nanodiscs are disk-shaped nanoscale phospholipid bilayers surrounded by molecules of the amphipathic alpha-helical protein MSP, which acts as a belt that limits the size of the disk (Fig. 7A, B).

The method was originally based on the use of human apolipoprotein ApoA1. High density lipoproteins are composed of lipids and cholesterol, and the main apolipoprotein ApoA1 can take on various structural forms. It is synthesized in the liver, then, from a lipid-free form, it gradually takes the form of a ball of lipids, cholesterol and cholesterol esters, passing through a temporary discoid stage. These discs became the prototype of water-soluble nanoparticles [87].

The incorporation of the membrane protein into the nanodiscs occurs spontaneously, since it interacts with hydrophobic lipid tails. Nanodiscs can be used over a wide concentration range at room and physiological temperatures and stored for several months at 4 ° C with minimal aggregation. Under the right conditions, monodisperse samples with a controlled size can be achieved compared to liposomes, bicelles, micelles. Currently, there are many modified variants of the MSP protein [88], including commercially available ones.

The quantitative and qualitative composition of nanodisc phospholipids can be varied to simulate the biological characteristics of certain membranes. The most popular synthetic lipids used to assemble nanodiscs are phosphatidylcholine (POPC), dimyristoylphosphatidylcholine (DMPC), dipalmitoylphosphatidylcholine (DPPC), and mixtures with charged phospholipids such as PI(4,5)P_2, phosphatidylserine (PS), phosphatidylserine (PS), phosphatidylethanolamine (PE).

The publications of many structures of ion channels isolated in nanodiscs over the past five years clearly indicate the success of the method (Table 1). New variants of nanodiscs have emerged, which are adapted, among other things, for large proteins and complexes [89, 90], since the size of the nanodisc can be of decisive importance for maintaining the native oligomeric state of the protein incorporated in the nanodiscs. Moreover, for many types of nanodiscs, optimized protocols have already been published [91] and the optimal molar ratios of the lipid mixture have been selected.

6.3. Lipodiscs

One of the recent methods for isolating proteins in a natural lipid environment is the use of a styrene and maleic acid copolymer (SMA). An important feature of this polymer is the ability to switch between linear and helical conformations depending on the pH and ionic strength of the medium. Alternating hydrophobic (styrene) and hydrophilic (maleic acid residues) fragments make it amphipathic, and therefore able to be embedded in biological membranes. Incorporating into the membrane, the polymer destroys it with formation of round membrane fragments of 10-40 nm in diameter, surrounded by a polymer belt [106] (Fig. 7B). These membrane fragments surrounded by polymer are called SMALP - Styrene Maleic Acid-lipid particles.

Lipodisq® term was introduced by Malvern Cosmeceutics Ltd. for proprietary polymer/lipid mixtures developed as vehicles for hydrophobic pharmacological substances. Currently, "lipodisc" or "native nanodisc" terms are mainly applied to disc-shaped membrane structures formed by polymers, as opposed to the term "nanodisc", which refers to structures formed by apolipoprotein derivatives (see above).

The effects of the polymer composition (the ratio of styrene and maleic acid moieties), the pH of the medium, and the ionic strength of the solution on the solubilization efficiency of the model membrane are studied in detail in ref [107]. The polymer remains soluble in the pH range of 7-9, and it begins to aggregate with a lower pH. However, a polymer with a ratio of styrene and maleic acid residues of 1.4:1 can tolerate the pH decrease to 4. The high ionic strength of the solution reduces the solubility of the polymer, but increases the efficiency of membranes solubilization. Interestingly, the diameter of the resulting lipodiscs depends more on the lipid composition of the membrane than on the characteristics of the polymer [108]. The length of the polymer molecules at a given ratio of styrene and maleic acid residues slightly affects the size of the particles, and much more affects their stability [109]. The size of the lipodiscs are affected by the mass ratio of lipid and polymer as shown on the model system of liposomes formed by a 9:1 mixture of POPC/POPG. After reaching a critical concentration of polymer required for complete destruction of the vesicles, a further increase of polymer concentration leads to a decrease in the size of lipodiscs [110].

The influence of the bilayer lipid composition on the kinetics of SMALP formation has been studied [111, 112]. It was shown that the length of the acyl chain of lipids has a slight effect on the size of lipodiscs, but determines the kinetics of SMALP formation. Bilayer packaging features are crucial for this process: the phase, membrane thickness, lateral pressure, charge density, temperature, and ionic strength of the solution. Thinner membranes with low lateral pressure, low surface charge density, and high NaCl concentrations dissolve faster and with a higher SMALP yield. It is shown that the polymer has no affinity for any specific lipids and the

ratio of lipids in SMALP remains the same as it was in the native membrane. The thermodynamics of the SMALP formation was investigated on model membranes in the work [113].

The effect of the lipid composition on SMALPs formation is reflected in the kinetics of eukaryotic cell solubilization: according to fluorescence microscopy, intracellular membranes in the presence of SMA are destroyed faster and more efficiently than the plasma membrane [114]. The slower destruction of the plasma membrane may be partly due to the presence of a large number of structural proteins.

If the polymer is added to the protein containing membrane, protein molecules became enclosed in the forming lipodiscs, that is, the protein is cut out of the membrane while preserving a certain layer of lipids surrounding the protein. This was initially demonstrated for liposomes formed by DMPC and containing bacteriorhodopsin [115]. Later, ABC transporters were extracted from the membrane fractions of various cell types [116], complex IV was extracted from the mitochondria of yeast cells [117], human voltage-gated potassium channel Kv7.1 was extracted from unfractionated eukaryotic cells [118] using the SMA copolymer. Membrane proteins enclosed in lipodiscs appear quite stable and can be purified and analyzed by different biochemical methods.

A significant advantage of using SMA is the complete absence of detergent in the protein purification protocol. As a result, the SMA- solubilized proteins can be extracted together with their natural lipid environment and ligands. This approach allows to increase the stability and maintain the functional activity of purified proteins and protein complexes, as has been shown for the human adenosine receptor A2A[119], voltage-gated potassium channel KcsA [120], AcrB *E.coli* transporter [121], photoreaction center (RC) from the purple bacterium *Rhodobacter (Rba.) sphaeroides* [122]. Often, SMA increases the overall yield of solubilized protein, and also allows for single-stage purification [116, 118]. Preserving annular lipids of proteins extracted with SMA copolymer opens up wide opportunities for analysis of their natural lipid environment and lipid-protein interactions [123-125]. Co-extraction of lipids with membrane proteins was used to determine the lipid composition of *Saccharomyces cerevisiae* membrane microdomains [126].

The advantages of the SMA copolymer for the membrane proteins solubilization make it promising tool in structural studies. Table 2 contains structures of proteins stabilized in lipodiscs published for the period 2018-2020. Despite the relatively small number of papers, studies of ion channels stabilized with SMA become popular and show subnanometer resolution of reconstructions.

7. Study of ion channel dynamics using X-ray free electron lasers

With the design of X-ray free-electron lasers (XFEL) and micro-focus stations on synchrotron radiation sources, serial crystallography becomes the most important method for the study of membrane proteins [131]. A new approach to the acquisition of the diffraction data allows structural information to be collected from nano- and micro crystals at room temperature with minimal impact of radiation due to ultra-fast data acquisition in a time shorter than the typical time of global radiation damage of a crystal. The combination of the enormous brightness of the flash over 10 W/cm^2 (focused on an area of about 100 nm^2) and a short duration of about 10 fs leads to the unique fundamental capabilities of this new tool in structural biology.

When trying to crystallize membrane proteins, they often tend to form very small micro- or nanometer crystals. The diffraction quality of such crystals is usually worse than that of soluble protein crystals of similar size. In such cases, a better resolution of the crystal structure can be achieved by increasing the power of the X-ray source, while the pulse length should be shorter than the characteristic time of crystal collapse, i.e. a few fs. Recently, the lipid cubic phase (LQP) was used for crystallization of membrane proteins [132]. This approach and the development of special injectors for viscous solutions made it possible to develop a method of serial femtosecond crystallography (Fig. 8A). It allows collecting diffraction data from multiple microcrystals, embedded in the LQP, with only one diffraction pattern per crystal in one orientation to be saved at the time. A large amount of such raw data is combined into one set. This method was instrumental to obtain structures of such ion channels as the GPCR-receptor [133] and bacteriorodopsin [134]. The light-induced isomerisation of bacteriorodopsin retinal is one of the fastest reactions in biology known, but recently the ultrafast photochemical reactions including light-induced molecular movements inside retinal within femtoseconds (Fig. 8B) has been observed with atomic resolution [134].

CONCLUSIONS

We are witnesses of the rapid developments in structural research of ion channels. Over the last 5 years, more than 50 new structures of various ion channels have been obtained with the help of cryo-EM, which is several times more than those obtained with the help of X-ray crystallography in recent 20 years. Cryo-EM revealed the reconstructions of such ion channels, as a glutamate receptor [135], that previously could not be crystallized in full due to their size and complex organization.

With the development of structural biology, electrophysiology has received new development and is used to validate new structures. As opposed to structural studies, functional research is easy to do in real time: opening and closing a channel takes milliseconds to seconds. Dynamics of cardiac channels activity are thus accessible, and combination of mutagenesis and

electrophysiology helps sorting out the functional relevance of structural data. This helps understanding the pathogenesis of channelopathies, diseases provoked by mutations in ion channels. As a recent and promising functional model, cardiomyocytes derived from induced pluripotent stem cells express many of the proteins that are present in mature cardiomyocytes, allowing a more physiological picture of the combined activity of tens of cardiac ion channels.

Structural studies so far have resulted in a discrete number of "frozen" conformations, which could only be set in motion by MD with a time limit of the order of μs. However, these limitations could also be overcome. With the development of XFEL, the time-resolved serial crystallography method has allowed dynamic patterns of ion channel activation to be obtained [134].

The work was supported by RFBR grants: 18-504-12045 (ion channels in SMA) and 20-54-15004 (structure and physiology of KCNE2 and KCNQ1 channels). Gildas Loussouarn has been supported by the CNRS grant PRC RUSSIE 2019 (PRC #2773).

.

Table 1. Ion channels whose structures are obtained in nanodiscs*.

Ion channel	year	MSP type	lipids	Structural method	resolution	ref
KCC4	2020	MSP1D1	DOPE, POPC, POPS	Cryo-EM	3.65 Å	[92]
VSD4-NavAb	2020	MSP1E3	DMPC	EM	-	[93]
KCNQ1 & KCNE3	2020	MSP2N2	Soybean polar lipids	Cryo-EM	3.1 Å	[94]
V/A-type ATPase	2019	MSP1E3D1	POPC and *T. thermophilus* polar lipids	Cryo-EM	3.5 Å	[95]

* abbreviations: dimiristoylglycerophosphorylglycerine (**DMPG**), palmitoyiloleoil-glycerophosphoglycerine (**POPG**), palmitoyiloleoilglycerophosphoethanolamine (**POPE**), 1-palmitoyiloleoyilglycerophosphoserine (**POPS**), Dioleoilphosphatidilethanolamine (**DOPE**).

TMEM16F	2019	MSP2N2	Soybean polar lipids, POPC, POPE, POPS	Cryo-EM	~ 4 Å	[96]
AdeB	2019	MSP 1E3D1	*E. coli* lipid extract	Cryo-EM	2.98 Å	[97]
LRRC8A	2019	MSP1E3D1	POPC	Cryo-EM	4.18 Å	[98]
H^+-ATPase	2019	MSP1E3D1	Yeast vacuolar lipids	EM	-	[99]
Orai	2019	MSP1E3D1	POPC, POPG, POPE	Cryo-EM	5.7 Å	[85]
TRPM4	2018	MSP2N2	Soybean polar lipids	Cryo-EM	~3 Å	[100]
OSCA1.2	2018	MSP2N2	Soybean polar lipids	Cryo-EM	3.1 Å	[88]
TPC1	2018	MSP E3D1 & saposineA	Soybean polar lipids	Cryo-EM	3.7 Å	[101]

Kv1.2–2.1	2018	MSP1E3D1	POPC, POPG, POPE	Cryo-EM	3.3 Å	[102]
VDAC-1	2018	DCND	POPC, POPG with cholesterol	EM	-	[90]
Kv7.1	2017	MSP2N2	no exogenic lipids	EM	2.5 nm	[103]
TcdA1	2016	MSP1D1	POPC	Cryo-EM	3.46 Å	[104]
TRPV1	2016	MSP2N2 & MSP1E3	Soybean polar lipids	Cryo-EM	No ligand – 3.2 Å, with agonist – 2.9 Å, with antagonist – 3.4 Å	[105]
CorA	2016	MSP1D1	POPC, POPG	Cryo-EM	3.8 Å	[102]

Table 2. Ion channels whose structures are obtained in SMA using cryo-EM.

Ion channel	year	resolution	ref
KimA (*Bacillus subtilis*)	2020	3.7 Å	[120]
ASIC1	2020	2.8 & 3.7 Å	[86]
AcrB (*Salmonella Typhimurium*)	2020	4.6 Å	[127]
AcrB (*E. coli transporter*)	2018	8.8 Å	[128]
AcrB (*E. coli*)	2018	3.2 Å	[129]
Alternative complex III (ACIII) (*Flavobacterium johnsoniae*)	2018	3.4 Å	[130]

Figure legends

Figure 1: Structure and functioning of the VD ion channels. (A) Schematic of one α-subunit of Kv channel. Transmembrane segments S1-S6 and pore loop P are marked. Charged Arg on the S4 segment are indicated by plus signs. VSD - voltage-sensing domain. B. Crystal structure of one α-subunit of channel Kv1.2 (PDB ID 2A79). (B) Schematic of cardiac AP. The arrows indicate the VD channels responsible for the different phases of AP. (D) Normal intervals for ECG and intervals for LQT and SQT syndromes.

Figure 2: The path towards the structure of the *Shaker* Kv channel. (A) 1992 - it is demonstrated that the channel forms tetramer [20]; (B) 1998 - data on the channel water pore; (B) by 1999 the structures of the pore domain (homologous channel KcsA [21]) and tetramerization domain were published [22]; (D) 2000 - Hypothesis of a 'hanging gondola' [23]; (D) 2001 - the first 3D EM structure of the *Shaker* channel [24] confirmed the above hypothesis; (E) 2005 - crystal structure of a chimeric full-size Kv1.1/1.2 channel in complex with **β**-subunit [25].

Figure 3: Two models of the connections between the voltage sensor and the pore subunits of the ion channel. A. Mechanistic model is typical for *Shaker* family channels. B. Ligand-receptor model is typical for EAG, ERG, KCNQ channels. The figure is adapted from [28].

Figure 4. (A) The crystal structure of the KcsA bacterial pH-dependent potassium channel allowed molecular modelling of the homologous channel. Three potassium ions are located in the outer and inner selective filter positions (S1 and S3) and in the center of the water cavity. (B) Alignment of the sequences of the KcsA, *Shaker* and the homologous CNG1 channel. (B) Modeling of the conformational changes upon opening and closing of the CNG1channel gate, based on MD data. From [33].

Figure 5: Transmembrane domain interactions in Kv channels according to X-ray crystallography and cryo-EM. (A) Kv1.1/1.2 channel [25]; (B) Kv10.1 channel [75]. At the bottom is a schematic representation of the interaction between pore domains and VSD.

Figure 6. Comparison of closed and open Kv channel structures. (A) Differences in the positions of the transmembrane part and adjasent to the pore cytoplasmic domains of the open channel Kv11.1 (dark grey) and closed channel Kv10.1 (light grey). (B) Comparison of pore

profiles for open (hERG and Kv1.2/2.1) and closed (EAG1) channels. (B) Model of EAG family channel activation. Adapted from [3].

Figure 7. Comparison of nanodisc and lipodisc complexes. Schematic representation of the nanodisc (A) and lipodisc (B) with incorporated membrane protein. At the bottom are the cryo-EM class-sum averages of the channels in the nano- and lipodisc: (B) dORAI channel in the MSP [85]. The arrow indicates the additional density corresponding to the nanodisc; (D) ASIC channel in SMA [86]. Note that the SMA does not form any extra-density around the membrane part of the channel, unlike the nanodisc.

Figure 8. Time-resolved serial femtosecond crystallography. (A) Installation setup. (B) Light-induced time-resolved isomerisation of bacteriorodopsin retinal (from [134]).

Figures

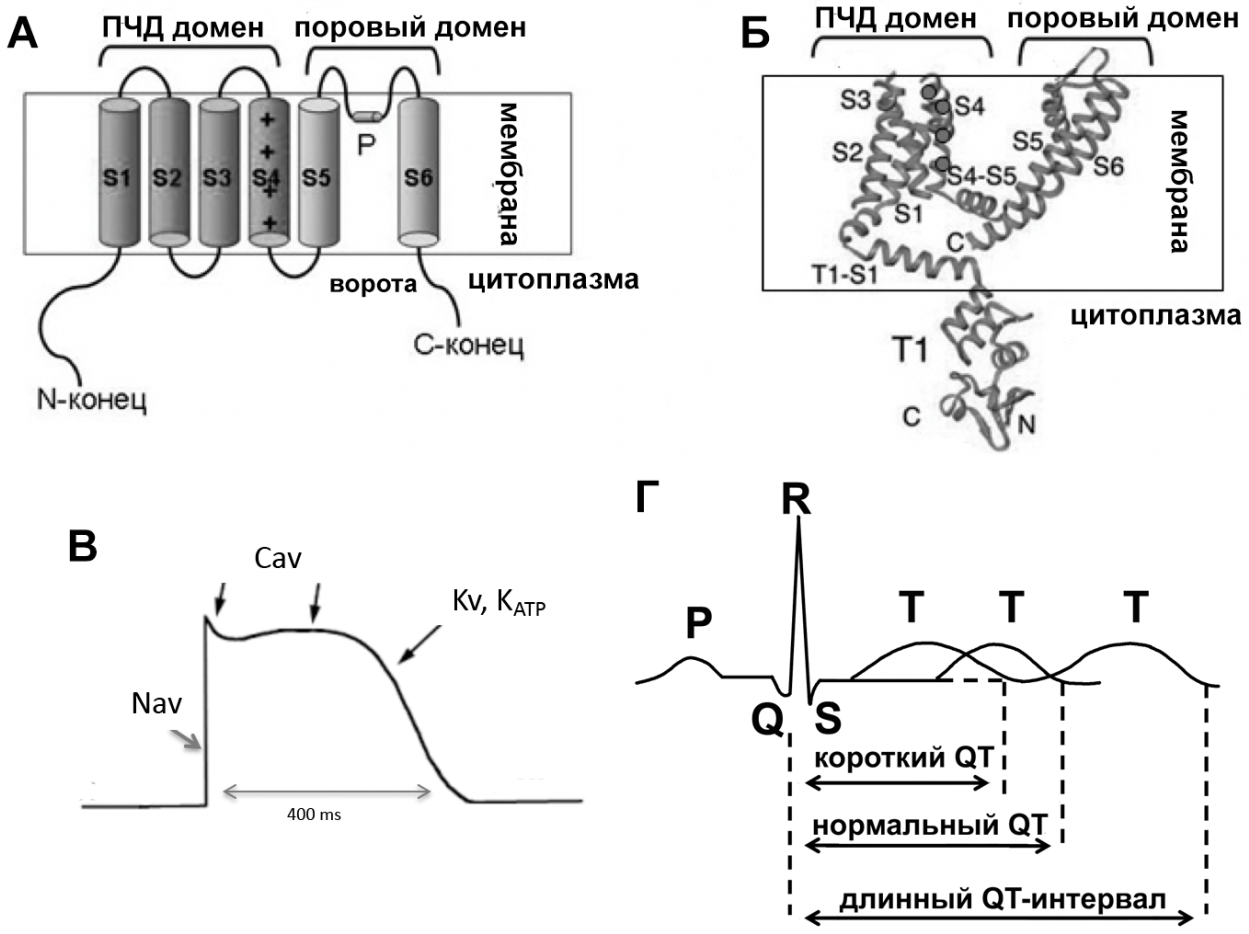

Рис 1

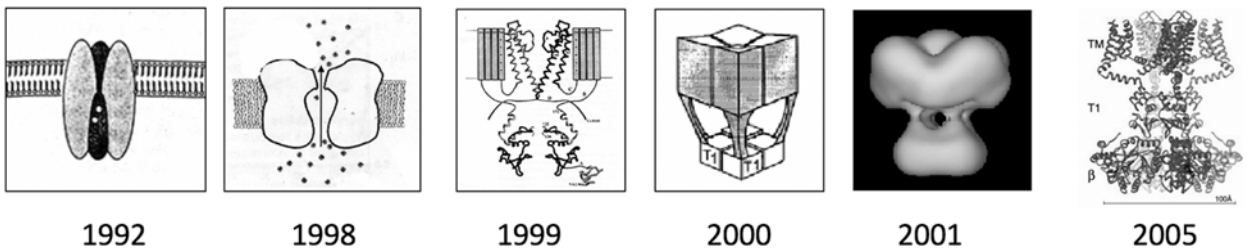

Рис 2

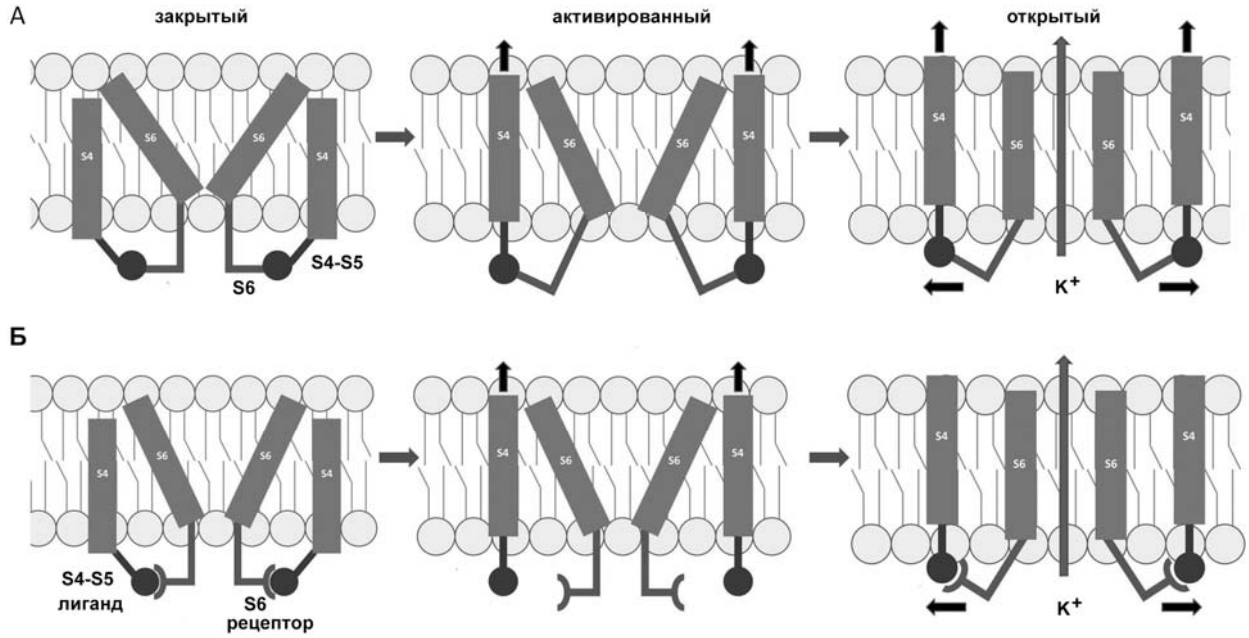
А
закрытый
активированный
открытый
S4
S6
S4-S5
K+
Б
S4-S5
лиганд
S6
рецептор

Рис 3

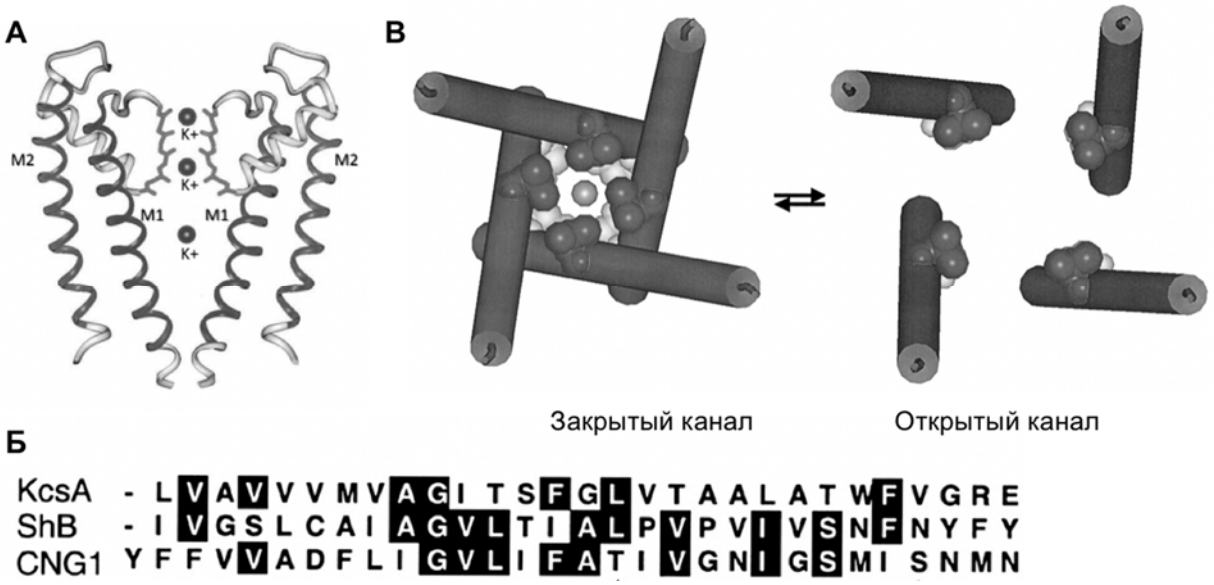
А
M2
M1
K+
В
Закрытый канал
Открытый канал
Б
KcsA - L V A V V V M V A G I T S F G L V T A A L A T W F V G R E
ShB - I V G S L C A I A G V L T I A L P V P V I V S N F N Y F Y
CNG1 Y F F V V A D F L I G V L I F A T I V G N I G S M I S N M N

Рис 4

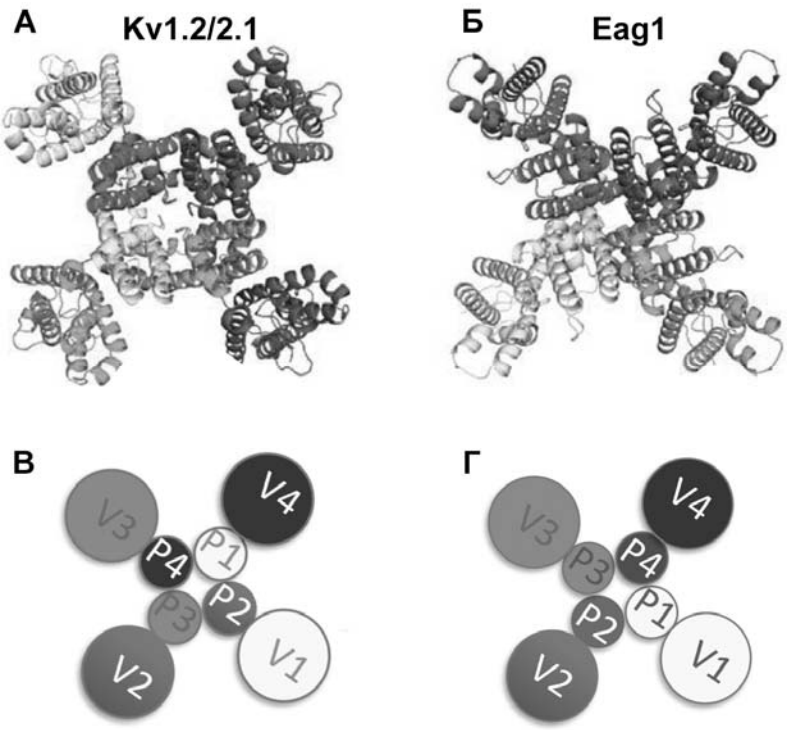
А
Kv1.2/2.1
Б
Eag1
В
V4
V3
P4
P1
P3
P2
V2
V1
Г
V4
V3
P4
P3
P2
P1
V2
V1

Рис 5

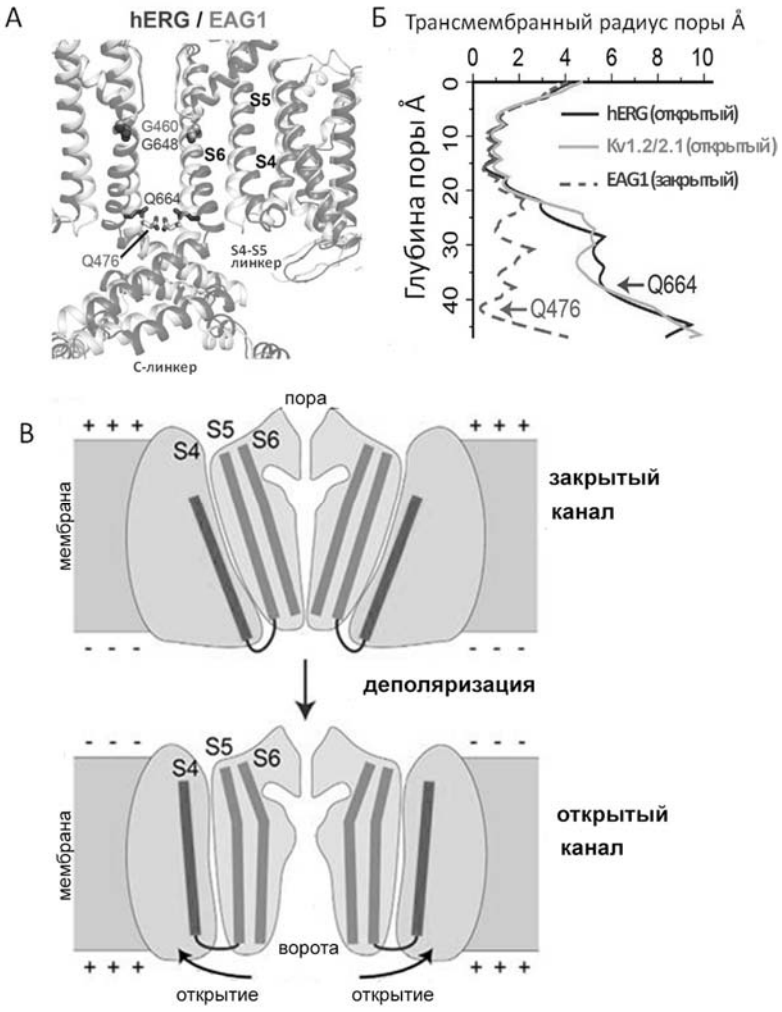
А
hERG / EAG1
S5
G460
G648
S6
S4
Q664
Q476
S4-S5
линкер
С-линкер
Б
Трансмембранный радиус поры Å
0 2 4 6 8 10
Глубина поры Å
0
10
20
30
40
hERG (открытый)
Kv1.2/2.1 (открытый)
EAG1 (закрытый)
Q664
Q476
В
пора
S5
S6
S4
мембрана
закрытый
канал
деполяризация
открытый
канал
ворота
открытие
открытие

Рис 6

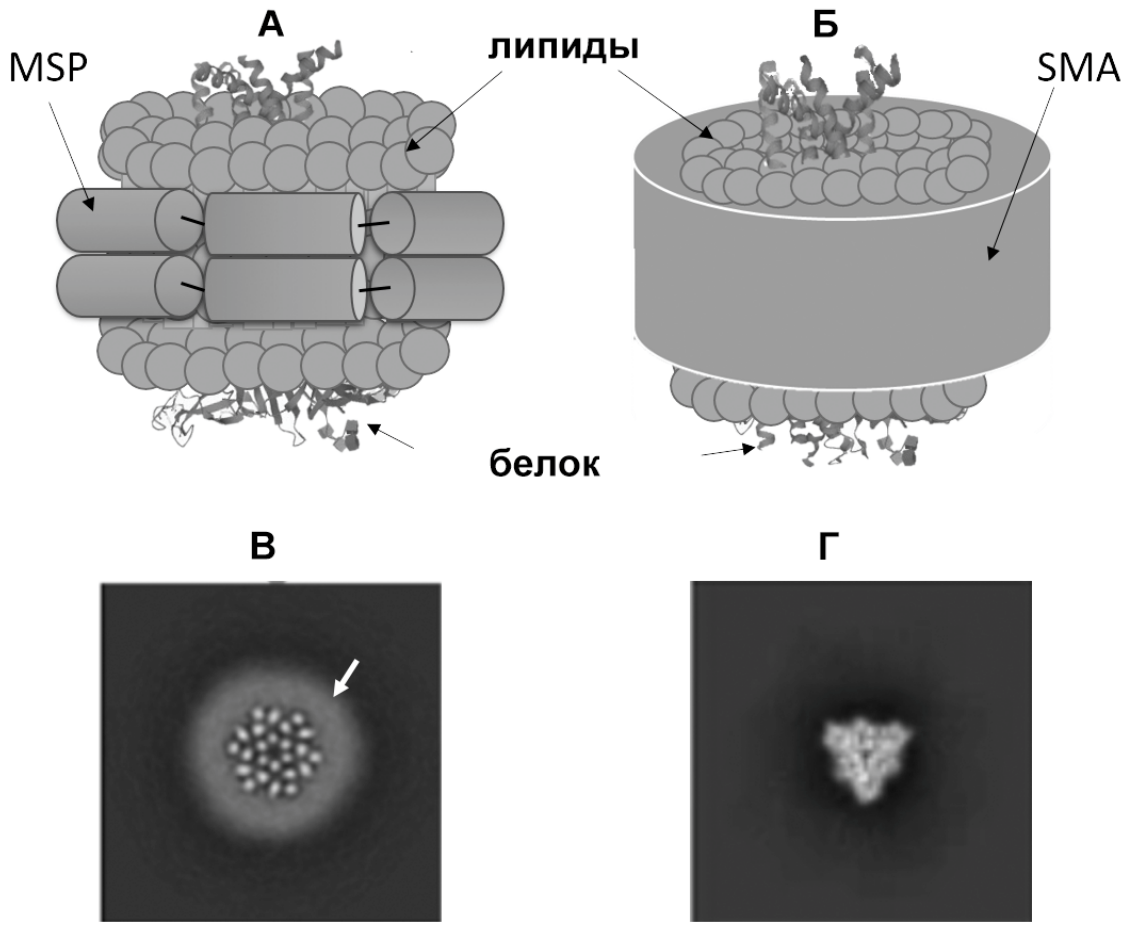
А
MSP
липиды
Б
SMA
белок
В
Г

Рис 7

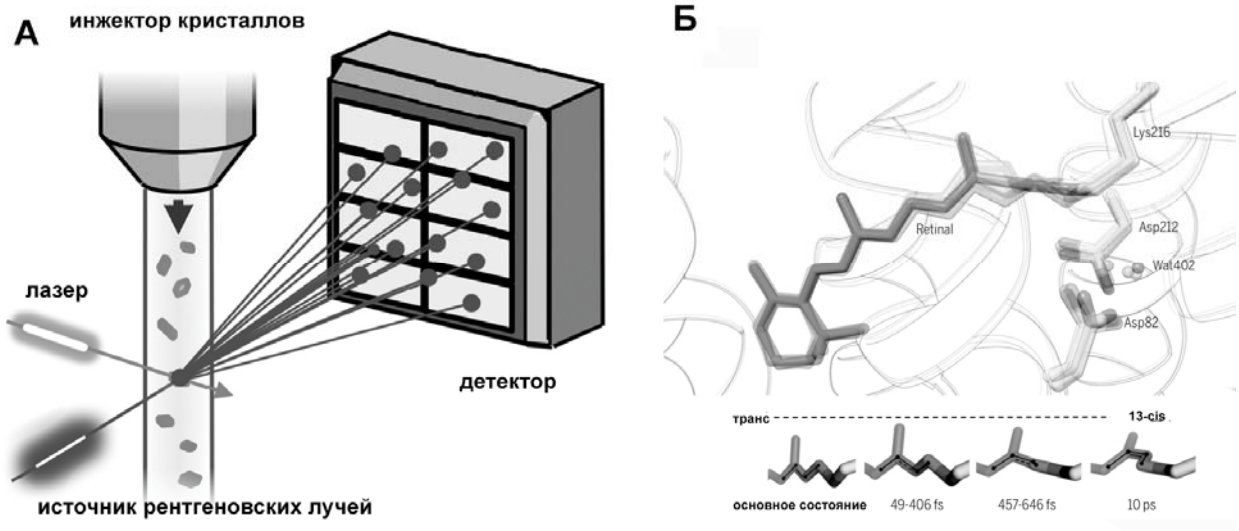
А
инжектор кристаллов
лазер
детектор
источник рентгеновских лучей
Б
Lys216
Retinal
Asp212
Wat402
Asp82
транс
13-cis
основное состояние
49-406 fs
457-646 fs
10 ps

Рис. 8

Literature

1. *Natchiar, S.K., et al. //* Nature, 2017. V. 551(7681). P 472-477.
2. *Suo, Y., et al. //* Neuron, 2020. V. 105(5). P 882-894.e5.
3. *Wang, W., R. MacKinnon* // Cell, 2017. V. 169(3). P 422-430.e10.
4. *Chakraborty, S., M. Jasnin, and W. Baumeister* // Protein Sci, 2020. V. 29(6). P 1302-1320.
5. *Owji, A.P, et al. //* Nat Struct Mol Biol, 2020. V. 27(4). P 382-391.
6. *Schmid, S. and T. Hugel* // Elife, 2020. V. 9.
7. *Jespersen, T., M. Grunnet, and S.P Olesen* // Physiology (Bethesda), 2005. V. 20. P 408-416.
8. *Peroz, D., et al. //* J Physiol, 2008. V. 586(7). P 1785-1789.
9. *Duggal, P, et al. //* Circulation, 1998. V. 97(2). P 142-146.
10. *Chen, Y.H., et al. //* Science, 2003. V. 299(5604). P 251-254.
11. *Smith, J.L., et al. //* J Arrhythm, 2016. V. 32(5). P 373-380.
12. *Koponen, M., et al. //* BMC Med Genet, 2018. V. 19(1). P 56.
13. *Tester, D.J., M.J. Ackerman* // Methodist Debakey Cardiovasc J, 2014. V. 10(1). P 29-33.
14. *Hu, D., et al. //* JACC Clin Electrophysiol, 2017. V. 3(7). P 727-743.
15. *Wang, Q.I., et al. //* J Cardiovasc Electrophysiol, 2014. V. 25(5). P 522-530.
16. *Hong, K., et al. //* J Cardiovasc Electrophysiol, 2005. V. 16(4). P 394-396.
17. *Hishigaki, H., S. Kuhara* // Database (Oxford), 2011. P bar017.
18. *Sanguinetti, M.C., et al. //* Novartis Found Symp, 2005. V. 266. P 159-166.
19. *Etheridge, S.P, S.Y. Asaki, M.C. Niu* // Curr Opin Cardiol, 2019. V. 34(1). P 46-56.
20. *Li, M., Y.N. Jan, L.Y. Jan* // Science, 1992. V. 257(5074). P 1225-1230.
21. *Doyle, D.A., et al. //* Science, 1998. V. 280(5360). P 69-77.
22. *Kreusch, A., et al. //* Nature, 1998. V. 392(6679). P 945-948.
23. *Kobertz, W.R., C. Williams, C. Miller* // Biochemistry, 2000. V. 39(34). P 10347-10352.
24. *Sokolova, O., L. Kolmakova-Partensky, N. Grigorieff* // Structure, 2001. V. 9(3). P 215-220.
25. *Long, S.B., E.B. Campbell, and R. Mackinnon* // Science, 2005. V. 309(5736). P 897-903.
26. *Grizel, A.V., G.S. Glukhov, O.S. Sokolova* // Acta Naturae, 2014. V. 6(4). P 10-26.
27. *Glauner K.S., Mannuzzu L.M., Gandhi C.S., Isacoff E.Y.* // Nature. 1999. V. 402(6763). P. 813. doi: 10.1038/45561. PMID: 10617202.
28. *Ferrer T, Rupp J, Piper DR, Tristani-Firouzi M.* // J Biol Chem, 2006 V.281(18). P 12858. doi: 10.1074/jbc.M513518200.
29. *Lee, S.Y., et al.* // Proc Natl Acad Sci U S A, 2005. V. 102(43). P 15441-1546.
30. *Yellen, G. //* Nature, 2002. V. 419(6902). P 35-42.
31. *Holyoake, J., et* al. // Eur Biophys J, 2004. V. 33(3). P 238-246.
32. *Jensen, M., et al. //* Science, 2012. V. 336(6078). P 229-233.
33. *Flynn, G.E., W.N. Zagotta* // Neuron, 2001. V. 30(3). P 689-698.
34. *MacKinnon, R., G. Yellen* // Science, 1990. V. 250(4978). P 276-279.
35. *Yool, A.J., T.L. Schwarz* // Nature, 1991. V. 349(6311). P 700-704.
36. *Liu, Y., et al. //* Neuron, 1997. V. 19(1). P 175-184.
37. *Schroeder, B.C., et al. //* Nature, 2000. V. 403(6766). P 196-199.
38. *Barhanin, J., et al. //* Nature, 1996. V. 384(6604). P 78-80.
39. *Sanguinetti, M.C., et al. //* Nature, 1996. V. 384(6604). P 80-83.
40. *Loussouarn, G., I. Baró, D. Escand* // Methods Mol Biol, 2006. V. 337. P 167-183.
41. *Keating, M.* // Circulation, 1992. V. 85(6). P 1973-1986.
42. *Tester, D.J., et al. //* Heart Rhythm, 2005. V. 2(5). P 507-517.
43. *Gourraud, J.B., et al. //* Front Cardiovasc Med, 2016. V. 3. P 9.
44. *Probst, V., et al. //* Circ Cardiovasc Genet, 2009. V. 2(6). P 552-557.

45. *Loussouarn, G., et al. //* EMBO J, 2003. V. 22(20). P 5412-5421.
46. *Rodriguez, N., et al. //* Biophys J, 2010. V. 99(4). P 1110-1118.
47. *Park, K.H., et al. //* Circ Res, 2005. V. 96(7). P 730-739.
48. *Choveau, F.S., et al. //* J Biol Chem, 2011. V. 286(1). P 707-716.
49. *Malak, O.A., Z. Es-Salah-Lamoureux, G. Loussouarn* // Sci Rep, 2017. V. 7(1). P 113.
50. *Malak, O.A., et al. //* J Biol Chem, 2019. V. 294(16). P 6506-6521.
51. *Malak, O.A., et al. //* Sci Rep, 2020. V. 10(1). P 5852.
52. *Ng, C.A., et al. //* Heart Rhythm, 2020. V. 17(3). P 492-500.
53. *Vanoye, C.G., et al. //* Circ Genom Precis Med, 2018. V. 11(11). P e002345.
54. *Takumi, T., H. Ohkubo, S. Nakanishi* // Science, 1988. V. 242(4881). P 1042-1045.
55. *Ben-Efraim, I., D. Bach, Y. Shai* // Biochemistry, 1993. V. 32(9). P 2371-2377.
56. *Lesage, F., et al. //* Receptors Channels, 1993. V. 1(2). P 143-152.
57. *van Huizen, R., et al. //* FEBS Lett, 1999. V. 457(1). P 107-111.
58. *Li, M., et al. //* Curr Biol, 1994. V. 4(2). P 110-115.
59. *Orlova, E.V., et al. //* J Mol Biol, 2003. V. 326(4). P 1005-1012.
60. *Sokolova, O., et al. //* Proc Natl Acad Sci U S A, 2003. V. 100(22). P 12607-12612.
61. *Wolf, M., et al. //* J Mol Biol, 2003. V. 332(1). P 171-182.
62. *Jiang, Q.X., D.N. Wang, R. MacKinnon* // Nature, 2004. V. 430(7001). P 806-810.
63. *Samsó, M., T. Wagenknecht, P.D. Allen* // Nat Struct Mol Biol, 2005. V. 12(6). P 539-544.
64. *Serysheva, I.I., et al. //* Proc Natl Acad Sci U S A, 2008. V. 105(28). P 9610-9615.
65. *Mishyna, M., et al. //* Micron, 2017. V. 96. P 57-64.
66. *Brilot, A.F., et al. //* J Struct Biol, 2012. V. 177(3). P 630-637.
67. *Corringer, PJ., et al. //* J Physiol, 2010. V. 588(Pt 4). P 565-572.
68. *Kuo, A., et al. //* Science, 2003. V. 300(5627). P 1922-1926.
69. *Jiang, Y., et al. //* Nature, 2003. V. 423(6935). P 33-41.
70. *Kawate, T., et al. //* Nature, 2009. V. 460(7255). P 592-598.
71. *Long, S.B., et al. //* Nature, 2007. V. 450(7168). P 376-382.
72. *Brohawn, S.G., J. del Mármol, R. MacKinnon* // Science, 2012. V. 335(6067). P 436-441.
73. *Liao, M., et al. //* Nature, 2013. V. 504(7478). P 107-112.
74. *Scheres, S.H.* // Methods Enzymol, 2016. V. 579. P 125-157.
75. *Whicher, J.R., R. MacKinnon* // Science, 2016. V. 353(6300). P 664-669.
76. *Sun, J., R. MacKinnon* // Cell, 2017. V. 169(6). P 1042-1050.e9.
77. *Jiang, Y., et al. //* Nature, 2003. V. 423(6935). P 42-48.
78. *Lörinczi, É., et al. //* Nat Commun, 2015. V. 6. P 6672.
79. *Ferrer, T., et al. //* J Biol Chem, 2006. V. 281(18). P 12858-12864.
80. *Schertler, G.F., C. Villa, R. Henderson* // Nature, 1993. V. 362(6422). P 770-772.
81. *Unwin, N. //* Nature, 1995. V. 373(6509). P 37-43.
82. *Jiang, Q.X., D.W. Chester, F.J. Sigworth* // J Struct Biol, 2001. V. 133(2-3). P 119-131.
83. *Antonenko, Y.N., et al. //* Phys Chem Chem Phys, 2015. V. 17(26). P 17461-17470.
84. *Marius, P, et al. //* Biophys J, 2005. V. 89(6). P 4081-9.
85. *Liu, X., et al. //* PLoS Biol, 2019. V. 17(4). P e3000096.
86. *Yoder, N., E. Gouaux* // Elife, 2020. V. 9.
87. *Peters-Libeu, C.A., et al. //* J Lipid Res, 2007. V. 48(5). P 1035-1044.
88. *Johansen, N.T., et al. //* FEBS J, 2019. V. 286(9). P 1734-1751.
89. *Zhao, Z., et al. //* J Am Chem Soc, 2018. V. 140(34). P 10639-10643.
90. *Nasr, M.L., et al. //* Nat Methods, 2017. V. 14(1). P 49-52.
91. *Hagn, F., M.L. Nasr, G. Wagner* // Nat Protoc, 2018. V. 13(1). P 79-98.
92. *Reid, M.S., D.M. Kern, S.G. Brohawn* // Elife, 2020. V. 9.
93. *Gardill, B., et al. //* Sci Rep, 2020. V. 10(1). P 1130.
94. *Sun, J., R. MacKinnon* // Cell, 2020. V. 180(2). P 340-347.e9.
95. *Zhou, L., L.A. Sazanov* // Science, 2019. V. 365(6455).
96. *Feng, S., et al. //* Cell Rep, 2019. V. 28(2). P 567-579.e4.

97. *Su, C.C., et al. //* mBio, 2019. V. 10(4).
98. *Kern, D.M., et al. //* Elife, 2019. V. 8.
99. *Sharma, S., et al. //* J Biol Chem, 2019. V. 294(16). P 6439-6449.
100. *Autzen, H.E., et al. //* Science, 2018. V. 359(6372). P 228-232.
101. *Kintzer, A.F., et al. //* Proc Natl Acad Sci U S A, 2018. V. 115(39). P E9095-E9104.
102. *Matthies, D., et al. //* Cell, 2016. V. 164(4). P 747-756.
103. *Shenkarev, Z.O., et al. //* Biochemistry (Mosc), 2018. V. 83(5). P 562-573.
104. *Gatsogiannis, C., et al. //* Nat Struct Mol Biol, 2016. V. 23(10). P 884-890.
105. *Gao, Y., et al. //* Nature, 2016. V. 534(7607). P 347-351.
106. *Tonge, S.R., B.J. Tighe* // Adv Drug Deliv Rev, 2001. V. 53(1). P 109-122.
107. *Scheidelaar, S., et al. //* Biophys J, 2016. V. 111(9). P 1974-1986.
108. *Colbasevici, A., et al. //* Biochim Biophys Acta Biomembr, 2020. V. 1862(5). P 183207.
109. *Domínguez Pardo, J.J., et al. //* Biophys J, 2018. V. 115(1). P 129-138.
110. *Zhang, R., et al. //* Biochim Biophys Acta, 2015. V. 1848(1 Pt B). P 329-333.
111. *Scheidelaar, S., et al. //* Biophys J, 2015. V. 108(2). P 279-290.
112. *Dominguez Pardo, J.J., et al. //* Eur Biophys J, 2017. V. 46(1). P 91-101.
113. *Cuevas Arenas, R., et al. //* Nanoscale, 2016. V. 8(32). P 15016-15026.
114. *Dörr, J.M., et al. //* Biochim Biophys Acta Biomembr, 2017. V. 1859(11). P 2155-2160.
115. *Knowles, T.J., et al. //* J Am Chem Soc, 2009. V. 131(22). P 7484-7485.
116. *Gulati, S., et al. //* Biochem J, 2014. V. 461(2). P 269-278.
117. *Long, A.R., et al. //* BMC Biotechnol, 2013. V. 13. P 41.
118. *Karlova, M.G., et al. //* Chem Phys Lipids, 2019. V. 219. P 50-57.
119. *Jamshad, M., et al. //* Biosci Rep, 2015. V. 35(2).
120. *Dörr, J.M., et al. //* Proc Natl Acad Sci U S A, 2014. V. 111(52). P 18607-18612.
121. *Postis, V., et al. //* Biochim Biophys Acta, 2015. V. 1848(2). P 496-501.
122. *Swainsbury, D.J., et al. //* Angew Chem Int Ed Engl, 2014. V. 53(44). P 11803-11807.
123. *Schmidt, V., et al. //* Biochim Biophys Acta Biomembr, 2019. V. 1861(2). P 431-440.
124. *Swainsbury, D.J.K., et al. //* Biochim Biophys Acta Bioenerg, 2018. V. 1859(3). P 215-225.
125. *Prabudiansyah, I., et al. //* Biochim Biophys Acta, 2015. V. 1848(10 Pt A). P 2050-2056.
126. *van 't Klooster, J.S., et al. //* Elife, 2020. V. 9.
127. *Parmar, M., et al. //* Biochim Biophys Acta Biomembr, 2018. V. 1860(2). P 378-383.
128. *Hernando, M., et al. //* Biochim Biophys Acta Biomembr, 2020. V. 1862(5). P 183191.
129. *Johnson, R.M., et al. //* Microorganisms, 2020. V. 8(6).
130. *Sun, C., et al. //* Nature, 2018. V. 557(7703). P 123-126.
131. *Standfuss, J. //* Curr Opin Struct Biol, 2019. V. 57. P 63-71.
132. *Caffrey M., Cherezov V.* // Nat Protoc, 2009, V. 4(5). P 706-731.
133. *Cherezov V., et al.* // Science. 2007, V. 318(5854). P 1258-1265.
134. *Nogly P. et al.* // Science, 2018. V. 361(6398). P. eaat0094.
135. *Twomey, E.C., A.I. Sobolevsky* // Biochemistry, 2018. V. 57(3). P 267-276.